RESEARCH OUTPUTS / RÉSULTATS DE RECHERCHE

High-Yield Synthesis of Ethyl Lactate with Mesoporous Tin Silicate Catalysts Prepared by an Aerosol-Assisted Sol–Gel Process

Godard, Nicolas; Vivian, Alvise; Fusaro, Luca; Cannavicci, Lorenzo; Aprile, Carmela; Debecker, Damien P.

Link to publication

Citation for pulished version (HARVARD):
Godard, N, Vivian, A, Fusaro, L, Cannavicci, L, Aprile, C & Debecker, DP 2017, 'High-Yield Synthesis of Ethyl Lactate with Mesoporous Tin Silicate Catalysts Prepared by an Aerosol-Assisted Sol–Gel Process', *ChemCatChem*, vol. 9, no. 12, pp. 2211-2218. https://doi.org/10.1002/cctc.201601637

Accepted Article

Authors: Nicolas Godard, Alvise Vivian, Luca Fusaro, Lorenzo Cannavicci, Carmela Aprile, and Damien P. Debecker

A Journal of

ChemPubSoc
Europe

FULL PAPER

High-yield synthesis of ethyl lactate with mesoporous SnSi mixed oxide catalysts prepared by the aerosol-assisted sol-gel process

Nicolas Godard,[b#] Alvise Vivian,[b#] Luca Fusaro,[b] Lorenzo Cannavicci,[a] Carmela Aprile, [b,*] Damien P. Debecker[a,*]

Abstract: An aerosol assisted sol-gel method is used to prepare mesoporous tin silicate catalysts which exhibit record activity in the synthesis of ethyl lactate from dihydroxyacetone and ethanol. The method is based on the formation of an aerosol from a solution of precursors and surfactant. During the fast drying of the droplets, the surfactant self-assembles and the Sn-silica matrix is formed by polycondensation reactions. After calcination, the resulting material is composed of a true Sn-Si mixed oxide in the form of spherical microparticles with calibrated mesopores of 5-6 nm. Tin species are incorporated in the silica network, mainly in the form of single sites. This makes these catalysts highly active for the targeted reaction, as shown by record turnover numbers. The catalyst is shown to be recyclable and truly heterogeneous, as it can be reused for several cycles and as it does not leach.

Introduction

Developments in catalysis science have often been triggered by innovation in the preparation of catalytic materials.[1] Of particular importance in the last decades is the advent of mesoporous catalytic materials, serving either as catalysts or catalyst supports with interesting structural and textural features.[2,3] As they exhibit pores in the 2-50 nm range as well as high specific surface area, mesoporous catalytic materials often allow both efficient mass transfer and high catalytic activities.

Bottom-up approaches, including sol-gel methods combined with templating strategies, are recognized as a powerful way to obtain tailored mesoporous materials with controlled composition, texture, and surface functionalities.[4,5] Typically, molecular precursors are first hydrolysed and then polycondensed in a medium that contains sacrificial structuring agents (organic micelles of surfactant, for example). Upon drying and calcination, the inorganic network is consolidated and the porosity is released.

Importantly, mixed oxides can be prepared using such sol-gel approaches, thereby incorporating directly the catalytically active element. In this case, a key parameter is the homogeneity of the mixed oxide. For example, the true incorporation of Al or Ti atoms in a silica network generates dehydration activity in

aluminosilicates[6,7] or epoxidation activity in titanosilicates.[8,9] Highly dispersed molybdates are recognized as the most active olefin metathesis active sites.[10] In biomass conversion, isolated sites of Sn oxides in silica catalyse important reactions like glucose isomerization[11] or alkyl lactate synthesis.[12,13]

In recent years, an aerosol-assisted sol-gel process[14,15] has emerged as an innovative, versatile and effective way to produce nanostructured porous catalysts exhibiting new properties and high performances.[16] In this synthesis process (Figure 1), the condensation of the inorganic network occurs during a short drying time, along with the evaporation-induced self-assembly of surfactant molecules serving as sacrificial template to generate pores. The method allows the formation of spherical particles with calibrated porosity and with a precise control on the composition and homogeneity of complex formulations.[17,18] The aerosol process can be run in a continuous mode and scaled up relatively easily to industrial scale.

Considering the importance of Sn-silicate in the topical context of biomass conversion, we turned our attention to the aerosol process for the preparation of catalysts dedicated to alkyl lactate synthesis.

With the advent of biodiesel, enormous excess of glycerol – a by-product of oil trans-esterification – is continuously poured on the market. As a consequence, crude glycerol is now considered as a waste and new solutions for its effective utilization are intensively being investigated.[19] Trioses, such as dihydroxyacetone (DHA), can be obtained from glycerol via catalytic means.[20–23] The subsequent synthesis of alkyl lactate from DHA and alcohol is the subject of intense research efforts. Indeed, both lactic acid and its esterification derivatives present important applications as green solvents and intermediates for the production of chemicals, pharmaceuticals, and cosmetic products.[24] Moreover, they are the precursors for the synthesis of polylactates, increasingly employed as a biodegradable plastic material.[25–27]

Transition metals as homogenous complexes and tin halides were found to catalyse effectively the synthesis of alkyl lactate from DHA.[28–30] However, the separation of homogeneous catalysts from the products and the use of heavy and toxic metals pose serious limitations to the sustainability of the process. Therefore, the development of highly active heterogeneous catalysts for a more sustainable process is of great interest.

It was recently reported that porous structured silica in the form of microporous crystalline solids (zeolites) or as mesoporous materials (e.g. MCM-41, SBA-15, TUD-1), with metallic elements

[a] Institute of Condensed Matter and Nanoscience - Université catholique de Louvain, Place Louis Pasteur, 1 box L4.01.09, 1348 Louvain-la-Neuve, Belgium.
[b] Unit of Nanomaterial Chemistry, University of Namur, Department of Chemistry, 5000 Namur, Belgium
[*] Corresponding authors: carmela.aprile@unamur.be ;
damien.debecker@uclouvain.be ;
[#] These authors contributed equally to the present work

Supporting information for this article is given via a link at the end of the document.
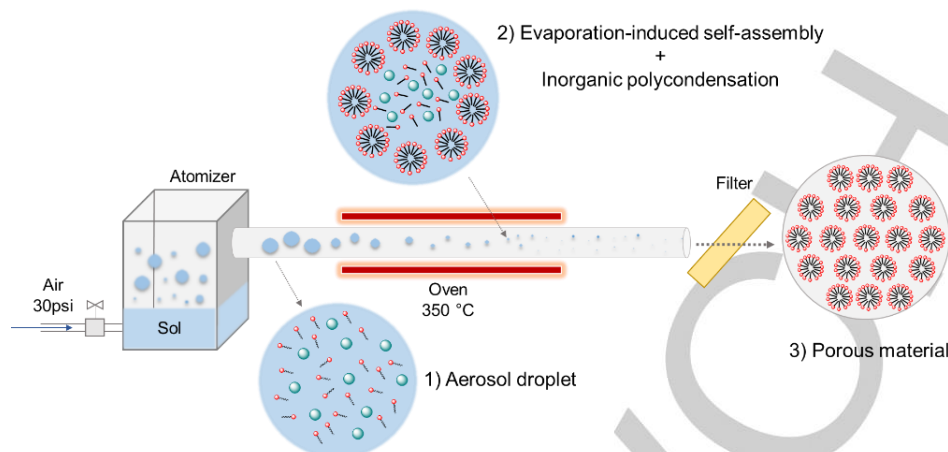
FULL PAPER

Figure 1. Schematic view of the aerosol-assisted sol-gel process.

inserted as single sites in the silica framework, can be active and selective catalysts for the conversion of trioses to alkyl lactates.[13,31–35]

In particular, Sn-silicates emerged as highly active heterogeneous catalysts for the direct conversion of DHA to ethyl lactate.[13,34] Catalytic activity is known to be brought about by a combination of Lewis and mild Brønsted acid sites.[36] Previous works showed that accessibility – dictated by texture and particle size – as well as Sn speciation are key factors for obtaining high activity. In this perspective, mesoporous catalysts with small particle size were synthesized by a controlled sol-gel route. Such materials provided short diffusion paths and demonstrated record activity levels.[13]

In this study, we harness the unique opportunities offered by the aerosol-assisted sol-gel process to prepare Sn-based catalysts that are even more active in the conversion of DHA to ethyl lactate.

Results and Discussion

Two different tin silicates (SnSi-74 and SnSi-37) were synthesized *via* the aerosol-assisted sol-gel process. The main advantage of this one-pot synthesis procedure, compared to the traditional sol-gel approaches, is related to the possible formation of a solid catalyst in a continuous way without additional hydrothermal treatments under static conditions. This advantage together with the low waste production, the relatively short synthesis time and the easy collection of the solid allow considering the catalyst preparation as a sustainable procedure.

The morphological and textural properties of the tin-silicates bearing respectively a silicon to tin ratio of 74 (SnSi-74) and 37 (SnSi-37) were first addressed via transition electron microscopy (TEM). The catalyst consists of particles with spherical morphology with size-calibrated mesopores of 5-6 nm visible down to the core of the spheres (Figures 2 and S1). The spherical shape of the solids is a reminiscence of the aerosol droplets from which the solvent evaporates during the drying step. The pores are a reminiscence of the P-123 surfactant micelles, removed by calcination after the drying step.

The particle size distribution was estimated through TEM measurements on 400 particles (Figures 3a and S2). Despite the presence of a minor amount of very large particles (diameter superior to 1000 nm), the majority of the porous spheres (90% of the measured particles) display a relatively narrow distribution and a small size with a particle diameter comprised between 140 nm and 380 nm.

The textural properties of the tin silicates were confirmed by N_2-physisorption measurements (Figure 3b). Both solids displayed a type-IV isotherm characterized by a H2 hysteresis loop typical of tubular-shaped pores open at both ends. BJH analysis, performed on the adsorption branch of the isotherm, evidenced a narrow pore size distribution (PSD) centred at 6.1 nm in good agreement with TEM observations. This regular PSD corresponds to the thermal removal of P-123 micelles used as structure directing agent.[18] Both tin silicate materials exhibit a high specific surface area and pore volume (Table 1) as well as a
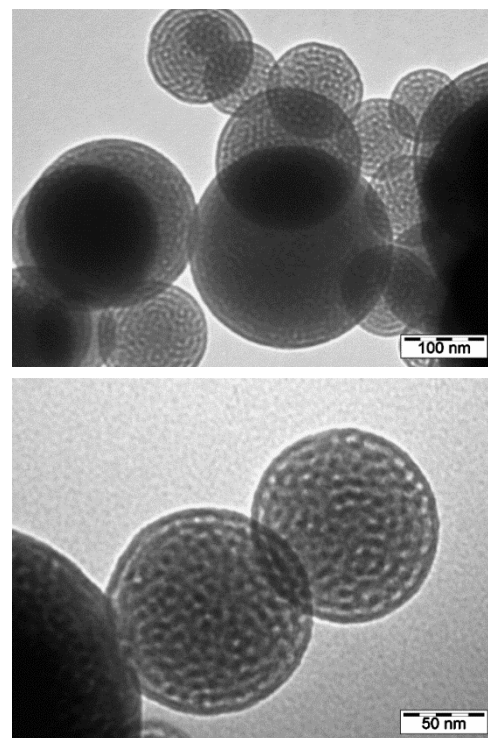

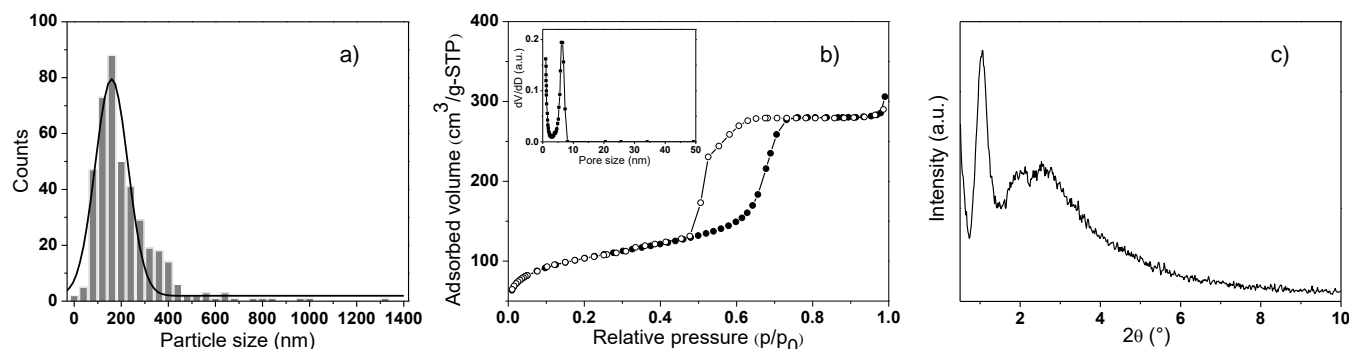**Figure 2.** TEM micrographs of SnSi-74 catalyst

FULL PAPER

Figure 3. Particle size distribution (a), Nitrogen adsorption/desorption isotherms and corresponding pore size distribution (insert) (b) and Small-angle XRD pattern of SnSi-74 catalyst (c)

minor contribution of microporosity corresponding to less than 10% of the total pore volume.

Small-angle XRD patterns (Figure 3c) revealed a sharp signal centred at $2\theta = 1.1°$ corresponding to the d_{100} reflection together with two smaller contributions due to the d_{110} and d_{200} reflections, confirming the presence of porous structures characterized by large mesopores and long range order. The structural and textural properties of the two solids are summarized in Table 1.

The chemical composition was verified by inductively coupled plasma optical emission spectroscopy (ICP-OES). The Si/Sn ratios for each material were in good agreement with the nominal composition (Table 1). The homogeneous distribution of Sn within the silica matrix was addressed through scanning electron transmission (SEM) using an energy dispersive X-ray (EDX) probe to map the samples (SI). This analysis allows excluding the presence of large separate domains of pure silica or tin oxides. However, in order to prove the insertion of Sn as single site within the silica framework additional characterization tools as Diffuse Reflectance UV-Vis and ^{119}Sn NMR spectroscopy are required.

Diffuse reflectance UV-visible spectroscopy (Figure 4) showed a main absorption band centred at 206 nm, which can be attributed to the presence of Sn(IV) in tetrahedral coordination within the silica architecture.[37,38] The presence of small contributions at higher wavelengths (240 and 280 nm respectively) can be assigned to distorted tetrahedral or penta-coordinated intra-framework Sn species.[38] In the literature, these two bands are also assigned to extra-framework SnO_2 clusters (240 nm) and hexa-coordinated polymeric Sn–O–Sn type domains (285 nm).[39] It is known that the synthesis of Sn silicates proceeds via hydrolysis of the precursors followed by condensation[40] with

consequent formation of Sn-O-Si and Si-O-Si bonds. The degree of condensation can be addressed via ^{29}Si NMR. Figure 5a shows the ^{29}Si CP-MAS (cross-polarization magic-angle spinning) spectrum of SnSi-74 material where the presence of Q^4 [$(SiO)_4Si$] (-111 ppm) and Q^3 [$(SiO)_3SiOH$] (-102 ppm) signals can be clearly observed. Due to the close proximity of Si atoms with hydroxyl groups in the Q^3 and Q^2 species, the intensities of Q^3 and Q^2 resonance lines are enhanced by the CP pulse sequence. Thus, the spectrum in Figure 5a was used to correctly assign the chemical shift of these two contributions, while for a quantitative evaluation a direct excitation experiment was performed as well.
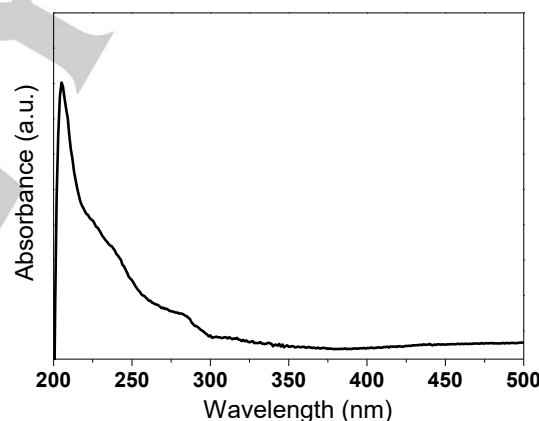
Figure 2. Diffuse reflectance UV–Vis spectrum of SnSi-74 catalyst

Table 1. Physicochemical properties of the SiSn mixed oxide catalysts

Material	Inter-reticular distance a_0 (nm)[a]	PSD (nm)	Wall (nm)[b]	Surface area (m^2 g^{-1})	Pore Vol. (cm^3/g)	Si/Sn ratio[c]
SiSn-74	9.6	6.1	3.5	360	0.48	79
SiSn-37	9.0	6.3	2.7	370	0.52	41

[a] Determined as $a_0 = 2d_{100}/\sqrt{3}$
[b] Determined as the difference between a_0 and the pore diameter
[c] Determined by ICP-OES

FULL PAPER

Figure 5. Solid State ^{29}Si MAS NMR spectra of SnSi-74 a) Cross Polarization, b) Direct Excitation

Figure 6. Solid state ^{119}Sn static NMR spectrum of SnSi-74 catalyst a) and pure SnO_2 b)

Thus, Figure 5b displays the quantitative ^{29}Si MAS NMR spectrum obtained by direct excitation of ^{29}Si. The deconvolution analysis using Gaussian functions of the Q^n contributions allows estimating the degree of condensation of the material: $Q^4/(Q^3+Q^2)$ = 2.2. This value indicates a degree of condensation in good agreement with the ones reported for standard silica based solid.[41]
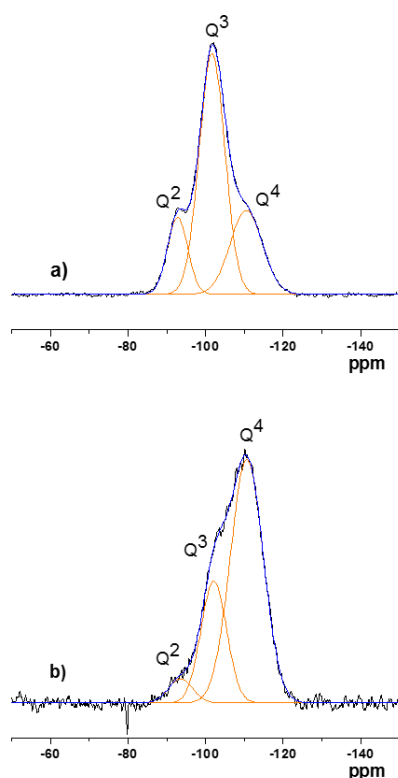
^{119}Sn-NMR performed under static conditions showed unambiguously that Sn was predominantly inserted in tetrahedral coordination. The signal centred at around –695 ppm (Figure 6a) can be attributed to intra-framework Sn(IV) connected to four silicon atoms via oxygen bridges[37,42] or partially hydrated tin species with an extended coordination shell.[42] The presence of significant amount of SnO_2 was not detected, since such extra-framework Sn(IV) species in octahedral coordination would yield a signal similar to that of pure SnO_2 nanoparticles (Figure 6b).[43,44] However, considering the broad linewidth of the signal in Figure 6a, the presence of minor amount of extra-framework SnO_2 cannot be completely excluded.

The catalyst displays a significant surface acidity, as probed by NH_3-TPD (Fig. S1). After adsorption of NH_3 at 50°C and flushing under inert, 220 μmol.g^{-1} of NH_3 desorb from SnSi-74 in two peaks centred at 120°C and 200°C, representative of weak and medium strength acid sites.

The catalyst with a higher Sn loading (SnSi-37) displayed very similar textural and structural properties. All the information as well as the complete characterization concerning this catalyst can be found in the supplementary information data (Fig. S2-S8).
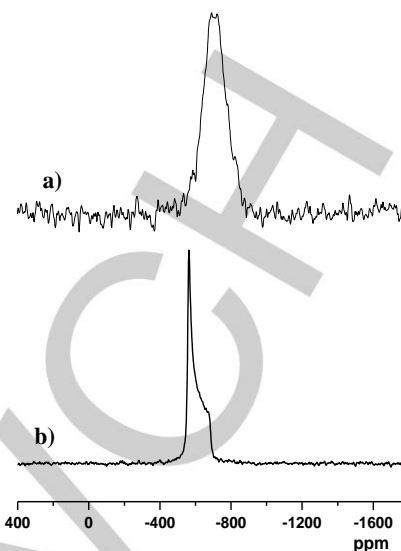
The previous characterization highlights the favourable features of these materials in the perspective of a catalytic applications. In particular, for the conversion of DHA to EL, the presence of Sn atoms inserted as single sites within the silica framework as well as the high surface area, the open mesoporosity, and possibly the small particle size are important requirements for a good activity. Thus, both SnSi-74 and SnSi-37 were tested as catalysts for the synthesis of ethyl lactate (EL).

The solids exhibited excellent catalytic performance in the conversion of dihydroxyacetone to ethyl lactate. The kinetic profiles of the conversion as a function of the time for the two solids are reported in Figure 7. As it can be seen, the selectivity toward EL increased with time. This observation is particularly evident for the catalyst displaying higher Sn loading (Figure 7b) and can be ascribed to the formation of the diethyl acetal as the main intermediate of the reaction. According to the literature, the proposed reaction mechanism[31] entails the formation of two main products: ethyl lactate and the diethyl acetal of pyruvic aldehyde. As suggested, the reaction starts with the formation of a pyruvic aldehyde intermediate, which can proceed towards the lactate by rearrangement and incorporation of an ethanol molecule or towards the acetal by addition of ethanol on strong Brønsted acid sites. It is known, that the isomorphic substitution of silicon with tin, generates a combination of Brønsted and Lewis acid sites,[13] thus explaining the presence of the intermediates.

Despite the modest selectivity of the reaction in the first 6 h, the kinetic profiles reported in Figure 7a show that the yield of EL increased with time while the yield of the intermediate tends to reach a plateau after 6 h of reaction. In the presence of SnSi-37 (Figure 7b) the yield of the intermediate species decreases after 6h of reaction and a selectivity higher than 80% can be achieved after 12h. This behaviour can be ascribed to the reversible formation of the diethyl acetal of pyruvic aldehyde under acid catalysis.[45]

Increasing the catalyst/reactant ratio, it is possible to push the reaction further. Almost total conversion of DHA with a 95% selectivity toward EL was achieved with SnSi-37 at 90 °C after 13
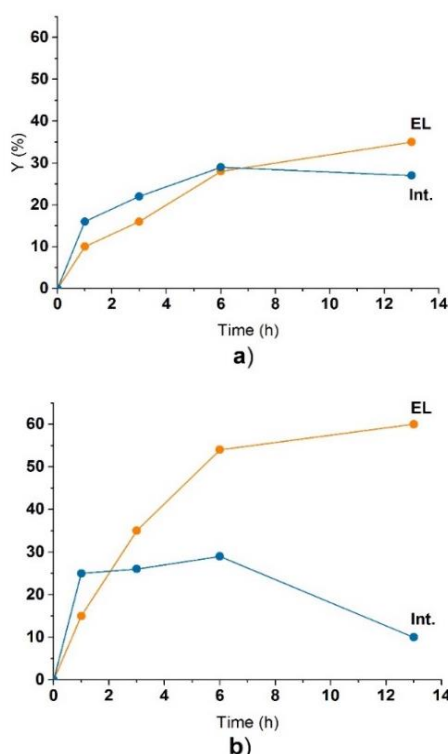
FULL PAPER

Figure 7. Kinetic study on SnSi-74 (a) and SnSi-37 (b). Conditions: 50 mg of catalyst, 5 mL of 0.2 M DHA solution in EtOH at 90 °C

h of reaction under appropriate conditions (100 mg of catalyst, 5 mL of DHA 0.2 M in ethanol).

Comparison with recently reported active catalysts was done at lower conversion (Table 2). In order to have a straightforward estimation of the activity of the different solids, turnover number (TON defined as mol DHA converted per mol of tin) was calculated as well. Moreover, the synthesis of one of the best catalysts previously reported in our research group (XS-Sn-MCM-41-A,[13] entry 3 in Table 2) was repeated and the solid was tested under the same reaction conditions employed for SnSi-74 and SnSi-37 (compare entries 1 to 3 in Table 2).

The tin silicates prepared via aerosol assisted procedure displayed better performance than the other tin based catalysts reported in the table. Moreover, both SnSi-74 and 37 clearly outcompete gallium and zinc silicates (compare entries 1 and 2 with 5 and 6). A direct comparison with other active catalysts reported in literature is difficult owing to the different reaction conditions in terms of temperature, reaction time, loading of active sites, alcohol used, substrate to catalyst ratio, etc. However, SnSi-74 displays better performances in terms of TON than other tin bases catalysts such as Sn-USY[46a] (TON = 58, calculated for the reaction between DHA and methanol, at 90°C, conversion after 5h) and Sn-beta[46b] (TON=120, calculated for the reaction between DHA and methanol at 80 °C, conversion after 24h) . As indicated by characterization data, the superior activity of the aerosol catalyst may be attributed to the good Sn dispersion and its effective incorporation in the silica network, generating abundant surface acid sites.

However, in the evaluation of a heterogeneous catalyst not only the activity but also the possibility of consecutive uses should be considered. SnSi-74 displayed excellent performance in the synthesis of ethyl lactate and it presented the best activity in terms of TON. It was hence selected for further investigations. The recyclability of SnSi-74 solid was tested in consecutives catalytic runs (Figure 8). Catalytic activity was maintained over 3 reaction runs, attesting of the good reusability of the catalysts. The slight decrease of TON in the third cycle could be ascribed to the presence of small amounts of organic species adsorbed on the surface of the material.

In order to further prove the stability of the solids under the selected reaction conditions, leaching tests were performed as well. In this experiment, DHA conversion was evaluated after 1 h of reaction (22 % conversion), the catalyst was removed *via* hot filtration and the filtrate was further allowed to react in the absence of catalyst and under the same reaction conditions for 5 h. The conversion remained practically unchanged during the additional 5h reaction (conversion = 23 % after 6h), demonstrating the absence of leaching of active sites and confirming that the catalytic reaction is truly heterogeneous (Figure 9).

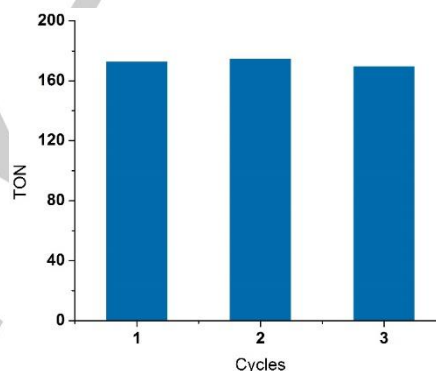**Figure 8.** Recycling test of SnSi-74 catalyst. Conditions: 50 mg of catalyst, 15 mL of 0.4 M DHA in EtOH, 6 h at 90 °C. TON calculated as mol of dihydroxyacetone converted per mol of Sn.
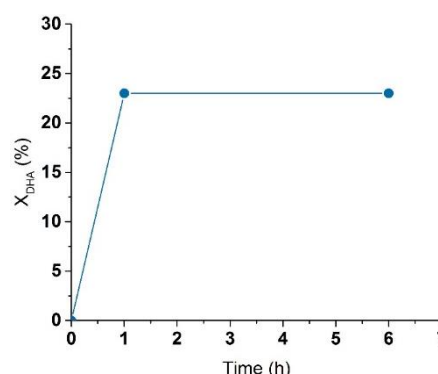

Figure 9. Leaching test of SnSi-74 catalyst. DHA conversion after 1h and 6h (catalyst removed). Conditions: 50 mg of catalyst, 5 mL of 0.4 M DHA in EtOH at 90 °C. Note: conversion after 6h in the presence of the catalyst reached 80%)

FULL PAPER

Table 2. Catalytic activity of the aerosol-made catalysts in the conversion of DHA to EL, and comparison with literature benchmarks.

Entry	Catalyst	Si/M	X_{DHA} (%)	Y_{EL} (%)	S_{EL} (%)	TON	Reference
1[a]	SnSi-74	79	34	12	36	173	This work
2[a]	SnSi-37	41	41	16	40	107	This work
3[a]	XS-Sn-MCM-41-A	63	24	15	63	113	This work
4	XS-Sn-MCM-41-A	65	24	15	69	117	Li *et al.*[13]
5	XS-Ga-MCM-41-H	15	20	12	60	9	Collard *et al.*[33]
6	XS-Zn-MCM-41-A	77	26	24	92	63	Collard *et al.*[32]
7	Sn-MCM-41	54	32	30	94	41	Li *et al.*[34]

[a]Conditions: 50 mg of catalyst, 15 mL of 0.4 M DHA in EtOH, 6 h at 90 °C.

Conclusions

In conclusion, novel mesoporous tin silicates were prepared via an easy, one-pot and continuous mode, using the aerosol-assisted sol-gel process. The synthesis of two solids (SnSi-37 and SnSi-74) bearing a different Sn loading was successfully achieved. The solids display interesting features for catalytic applications such as high surface area, regular mesoporosity and a successful incorporation of isolated Sn within the silica framework. These aerosol-made mesoporous Sn-silicates showed excellent catalytic performance in the conversion of dihydroxyacetone to ethyl lactate. The best catalyst displayed higher turnover number than the reference catalysts previously reported in literature. The catalysts do not leach and truly act in a heterogeneous mode. Moreover, it was successfully used in multiple catalytic cycles thus proving its stability under the selected reaction conditions.

Experimental Section

Materials

Pluronic® P-123, Hydrochloric acid (37%), tetraethyl orthosilicate (TEOS purity ≥99.99%) and tin (IV) chloride pentahydrate ($SnCl_4 \cdot 5H_2O$ purity 98.0%) were all purchased from Sigma–Aldrich. Absolute ethanol (Analytical grade) was purchased from Fisher Scientific.

Catalyst preparation

Solution **A** was prepared by hydrolyzing 12 g of tetraethyl orthosilicate (TEOS) in an aqueous solution (20 g) at pH 2 (HCl, 0.01 M). Pluronic® P123 (3.9 g) was dissolved in absolute ethanol (45 g) and acid aqueous solution (pH 2, 8 g) to yield solution **B**. Both solutions were left stirring overnight at room temperature and then tin (IV) chloride ($SnCl_4 \cdot 5H_2O$) was added to solution **A** in order to have a Si/Sn molar ratio equal to 74 or 37. Solutions **A** and **B** were mixed together and then stirred for 30 minutes. The clear solution obtained was atomized with a 6-Jet 9306A atomizer from TSI and the aerosol was dried by passing through a tubular quartz tube heated at 350 °C (Fig. 1a). The dried powders were collected on a cellulose nitrate filter, aged at 80°C for one night and calcined under static air at 550 °C for 6 h (heating rate of 1 °C/min). Samples are denoted SnSi-x, where 'x' is the atomic Si/Sn ratio.

Characterization

Transmission electron microscopy (TEM) images were taken using a Philips Tecnai 10 microscope operating at 80 kV. Nitrogen adsorption-desorption analyses were carried out at 77 K with a volumetric adsorption analyser (Micromeritics Tristar 3000). Prior to the analysis, the samples were pre-treated at 150 °C for 16 h under reduced pressure (0.1 mbar). The Brunauer–Emmet–Teller (BET) method was applied in the 0.05-0.30 P/P_0 range to calculate the specific surface area, while the pore size distributions were calculated from the adsorption isotherm using the Barrett–Joyner–Halenda (BJH) method. Powder X-ray diffraction (XRD) patterns were recorded on a PANalytical X'pert diffractometer with Cu Kα radiation (k = 1.54178 Å). Scanning electron microscopy (SEM) analysis was carried out on a JEOL 7500F scanning electron microscope. Energy-dispersive X-ray (EDX) spectroscopy was performed using an acceleration voltage of 15 kV. Inductively coupled plasma optical emission spectroscopy was employed to determine the chemical composition of the materials using an Optima 8000 ICP-OES Spectrometer. Diffuse reflectance UV–Vis spectra were collected on a Varian Cary 5000 UV–Vis–NIR Spectrophotometer with a Harrick single-beam Praying Mantis Diffuse Reflectance collection system. The Si environment and the coordination of the Sn atoms were studied by ^{29}Si Magic Angle Spinning (MAS-NMR) and static ^{119}Sn Nuclear Magnetic Resonance.

^{29}Si NMR spectra were recorded at room temperature on a Bruker Avance-500 spectrometer operating at 11.7 T (99.3 MHz for ^{29}Si) using a 4mm CP-MAS Bruker probe. The sample was packed in a 4 mm zirconia rotor and measured with a spinning frequency of 8000 Hz. Quantitative ^{29}Si spectra were recorded using the following acquisition parameters: 300s relaxation delay, 3µs (90°) excitation pulse, 52 ms acquisition time. CP-MAS spectra were recorded using a 5 s relaxation delay and 5 ms contact time. The processing comprised exponential multiplication of the FID with a line broadening factor of 30 Hz, zero-filling, Fourier transform, phase and baseline corrections. The chemical shift scale was calibrated at room temperature with respect to a sample of solid 3-(Trimethylsilyl)-1-propanesulfonic acid sodium salt (DSS) (0.0 ppm).

^{119}Sn NMR spectra were recorded at room temperature on a Varian VNMRS-400 spectrometer operating at 9.4 T (149 MHz for ^{119}Sn) using a 5mm wideline probe. The sample was packed in a 5 mm glass tube and studied in static condition. ^{119}Sn spectra were recorded using the Hahn echo pulse sequence and following acquisition parameters: 60s relaxation delay, 1.5µs (90°) excitation pulse, 5 ms acquisition time. The processing comprised exponential multiplication of the FID with a line broadening factor of 1000 Hz, zero-filling, Fourier transform, phase and baseline corrections. The chemical shift scale was calibrated at room temperature with respect to the isotropic shift of SnO_2 to -603 ppm.[47]

Acidity was studied by NH_3-TPD. Around 50 mg of sample was introduced in a quartz reactor on a Hiden Analytical Catlab-PCS apparatus. Prior to measurement, the sample was preheated in a dry air flow (30 ml.min^{-1}) at

FULL PAPER

550°C for 2 hours. Subsequently, it was cooled down to 50°C and then exposed to a gaz mixture of 5% NH$_3$ in He (10 ml.min^{-1}) and Ar (20 ml.min^{-1}) for 45 min. Physisorbed NH$_3$ was removed by purging with Ar (30 ml.min^{-1}) at 50°C for 90 min. The TPD measurement was conducted by heating the sample from 50 to 650°C with ramping rate of 5°C.min^{-1}. Desorbed NH$_3$ was detected by a mass spectrometer (QGA model).

Production of ethyl lactate from dihydroxyacetone

The catalytic tests were performed in batch mode using a reflux apparatus. In a typical experiment for the conversion of dihydroxyacetone (DHA) to ethyl lactate (EL), 540 mg of DHA (6 mmol, in the form of 1,3-dihydroxyacetone dimer) and 75 mg of nonane (0.58 mmol, as GC internal standard) were dissolved in 11.76 g of absolute ethanol (as solvent and reactant) at 45 °C for 30 min. Then, the selected amount of catalyst was added to the solution at room temperature. The reaction mixture was heated at 90 °C under vigorous stirring (1200 rpm) for the selected reaction time. At the end of the test, the catalyst was separated by centrifugation and the solution was analysed by gas chromatography (GC) on a Trace GC Ultra from Interscience. Recycling tests were performed by separating the catalyst from the reaction mixture by centrifugation followed by washing with ethanol (2 x 10mL). Finally, the catalyst was dried overnight at 100 °C. The catalyst was finally calcined in air at 500 °C for 2h (heating rate 2 °C/ min). Leaching tests were carried out under the general reaction conditions employed for the catalytic tests (vide supra). The catalyst was removed from the reaction mixture after 30 min by centrifugation, followed by hot filtration at the same temperature used for the catalytic test. The filtrate was allowed to react for another 5 h 30 min. The products were analysed by GC both after 1 h and at the end of the test (6h).

Acknowledgements

Keywords: mesoporous mixed oxide • sol-gel chemistry • EISA • spray drying • ethyl lactate

References

[1]   G. Busca in *Heterogeneous Catalytic Materials, Ch. 6,* Elsevier, **2014**, pp. 103–195.
[2]   C. T. Kresge, M. E. Leonowicz, W. J. Roth, J. C. Vartuli, J. S. Beck, *Nature* **1992**, *359*, 710–712.
[3]   N. Pal, A. Bhaumik, *RSC Adv.* **2015**, *5*, 24363–24391.
[4]   G. J. D. A. A. Soler-Illia, C. Sanchez, B. Lebeau, J. Patarin, *Chem. Rev.* **2002**, *102*, 4093–4138.
[5]   P. Yang, *Science (80-.)* **1998**, *282*, 2244–2246.
[6]   D. P. Debecker, C. Boissière, G. Laurent, S. Huet, P. Eliaers, C. Sanchez, R. Backov, *Chem. Commun.* **2015**, *51*, 14018–21.
[7]   S. K. Jana, H. Takahashi, M. Nakamura, M. Kaneko, R. Nishida, H. Shimizu, T. Kugita, S. Namba, *Appl. Catal. A Gen.* **2003**, *245*, 33–41.
[8]   Y. Jiang, Y. Zhao, X. Xu, K. Lin, D. Wang, *RSC Adv.* **2016**, *6*, 77481–77488.
[9]   K. Lin, O. I. Lebedev, G. Vana Tendeloo, P. A. Jacobs, P. P. Pescarmona, *Chem. - A Eur. J.* **2010**, *16*, 13509–13518.
[10]   D. P. Debecker, B. Schimmoeller, M. Stoyanova, C. Poleunis, P. Bertrand, U. Rodemerck, E. M. Gaigneaux, *J. Catal.* **2011**, *277*, 154–163.
[11]   R. Bermejo-Deval, M. Orazov, R. Gounder, S. J. Hwang, M. E. Davis, *ACS Catal.* **2014**, *4*, 2288–2297.
[12]   S. Tolborg, I. Sádaba, C. M. Osmundsen, P. Fristrup, M. S. Holm, E. Taarning, *ChemSusChem* **2015**, *8*, 613–617.
[13]   L. Li, X. Collard, A. Bertrand, B. F. Sels, P. P. Pescarmona, C. Aprile, *J. Catal.* **2014**, *314*, 56–65.
[14]   C. Boissiere, D. Grosso, A. Chaumonnot, L. Nicole, C. Sanchez, *Adv. Mater.* **2011**, *23*, 599–623.
[15]   Y. Lu, H. Fan, A. Stump, T. L. Ward, T. Rieker, C. J. Brinker, *Nature* **1999**, *398*, 223–226.
[16]   D. P. Debecker, M. Stoyanova, F. Colbeau-Justin, U. Rodemerck, C. Boissiãre, E. M. Gaigneaux, C. Sanchez, *Angew. Chemie - Int. Ed.* **2012**, *51*, 2129–2131.
[17]   F. Colbeau-Justin, C. Boissière, A. Chaumonnot, A. Bonduelle, C. Sanchez, *Adv. Funct. Mater.* **2014**, *24*, 233–239.
[18]   D. P. Debecker, M. Stoyanova, U. Rodemerck, F. Colbeau-Justinc, C. Boissère, A. Chaumonnot, A. Bonduelle, C. Sanchez, *Appl. Catal. A Gen.* **2014**, *470*, 458–466.
[19]   M. Pagliaro, R. Ciriminna, H. Kimura, M. Rossi, C. Della Pina, *Angew. Chemie - Int. Ed.* **2007**, *46*, 4434–4440.
[20]   S. Hirasawa, Y. Nakagawa, K. Tomishige, A. Corma, S. Iborra, A. Velty, P. Gallezot, M. Schlaf, R. M. West, E. L. Kunkes, et al., *Catal. Sci. Technol.* **2012**, *2*, 1150.
[21]   G. M. Lari, C. Mondelli, J. Pérez-Ramírez, *ACS Catal.* **2015**, *5*, 1453–1461.
[22]   A. Villa, S. Campisi, C. E. Chan-Thaw, D. Motta, D. Wang, L. Prati, *Catal. Today* **2015**, *249*, 103–108.
[23]   G.-Y. Yang, S. Shao, Y.-H. Ke, C.-L. Liu, H.-F. Ren, W.-S. Dong, *RSC Adv.* **2015**, *5*, 37112–37118.
[24]   M. Dusselier, P. Van Wouwe, A. Dewaele, E. Makshina, B. F. Sels, *Energy Environ. Sci.* **2013**, *6*, 1415–1442.
[25]   J. Coombs, K. Hall, *Renew. Energy* **1998**, *15*, 54–59.
[26]   R. A. Gross, B. Kalra, C. Bastoli, R. A. Gross, J.-D. Gu, D. Eberiel, S. P. McCarthy, C. M. Buchanan, B. G. Pearcy, A. W. White, et al., *Science* **2002**, *297*, 803–7.
[27]   L.-T. Lim, R. Auras, M. Rubino, *Prog. Polym. Sci.* **2008**, *33*, 820–852.
[28]   E. Bang, J. Eriksen, L. Mønsted, O. Mønsted, *Acta Chem. Scand.* **1994**, *48*, 12–19.
[29]   J. Eriksen, O. Mønsted, L. Mønsted, *Transition. Met. Chem.* **1998**, *23*, 783–787.
[30]   Y. Hayashi, Y. Sasaki, *Chem. Commun. (Camb).* **2005**, 2716–2718.
[31]   P. P. Pescarmona, K. P. F. Janssen, C. Delaet, C. Stroobants, K. Houthoofd, A. Philippaerts, C. De Jonghe, J. S. Paul, P. A. Jacobs, B. F. Sels, *Green Chem.* **2010**, *12*, 1083–1089.
[32]   X. Collard, P. Louette, S. Fiorilli, C. Aprile, *Phys. Chem. Chem. Phys.* **2015**, *17*, 26756–26765.
[33]   X. Collard, L. Li, W. Lueangchaichaweng, A. Bertrand, C. Aprile, P. P. Pescarmona, *Catal. Today* **2014**, *235*, 184–192.
[34]   a) L. Li, C. Stroobants, K. Lin, P. A. Jacobs, B. F. Sels, P. P. Pescarmona, *Green Chem.* **2011**, *13*, 1175–1181; b) L. Li, D. Cani, P. P. Pescarmona, *Inorganica Chim. Acta* **2015**, *431*, 289–296.
[35]   P. Y. Dapsens, C. Mondelli, J. Pérez-Ramirez, *Chem. Soc. Rev.* **2015**, *44*, 7025-7043.
[36]   F. De Clippel, M. Dusselier, R. Van Rompaey, P. Vanelderen, J. Dijkmans, E. Makshina, L. Giebeler, S. Oswald, G. V. Baron, J. F. M. Denayer, et al., *J. Am. Chem. Soc.* **2012**, *134*, 10089–10101.
[37]   K. Chaudhari, T. K. Das, P. R. Rajmohanan, K. Lazar, S. Sivasanker, A. J. Chandwadkar, *J. Catal.* **1999**, *183*, 281–291.
[38]   E. A. Alarcón, A. L. Villa, C. M. de Correa, *Microporous Mesoporous Mater.* **2009**, *122*, 208–215.
[39]   R. Bermejo-Deval, R. Gounder, M. E. Davis, *ACS Catal.* **2012**, *2*, 2705–2713.
[40]   P. Mulvaney, F. Grieser, D. Meisel, *Langmuir* **1990**, *6*, 567–572.
[41]   M. Luhmer, J. B. D'Espinose, H. Hommel, A. P. Legrand, *Magn. Reson. Imaging* **1996**, *14*, 911–913.
[42]   M. Renz, T. Blasco, A. Corma, V. Fornés, R. Jensen, L. Nemeth, *Chem. - A Eur. J.* **2002**, *8*, 4708–4717.
[43]   N. Kishor Mal, V. Ramaswamy, S. Ganapathy, A. V. Ramaswamy, *Appl. Catal. A, Gen.* **1995**, *125*, 233–245.
[44]   P. Shah, A. V. Ramaswamy, K. Lazar, V. Ramaswamy, *Microporous Mesoporous Mater.* **2007**, *100*, 210–226.
[45]   P. Y. Bruice, *Organic Chemistry*, Pearson Prentice Hall, **2007**.
[46]   a) X. Yang, L. Wu, Z. Wang, J. Bian, T. Lu, L. Zhou, C. Chen, J. Xu, *Catal. Sci. Technol.* **2016**, *6*, 1757-1763; b) E. Taarning, S. Saravanamurugan, M. Spangsberg Holm, J. Xiong, R. M. West, C. H. Christensen, *ChemSusChem* **2009**, *2*, 625-627.
[47]   C. Cossement, J. Darville, J. M. Gilles, J. B. Nagy, C. Fernandez, J. P. Amoureux, *Magn. Reson. Chem.* **1992**, *30(3)*, 263-270.
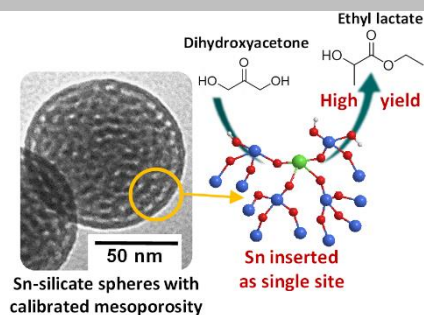
WILEY-VCH

FULL PAPER

Entry for the Table of Contents (Please choose one layout)

Layout 1:

FULL PAPER

An aerosol assisted sol-gel method is used to prepare mesoporous tin silicate catalysts which exhibit record activity in the synthesis of ethyl lactate from dihydroxyacetone and ethanol.

Sn-silicate spheres with calibrated mesoporosity

Nicolas Godard,[b#] Alvise Vivian,[b#] Luca Fusaro,[b] Lorenzo Cannavicci,[a] Carmela Aprile, [b,*] Damien P. Debecker[a,*]

Page No. – Page No.

High-yield synthesis of ethyl lactate with mesoporous SnSi mixed oxide catalysts prepared by the aerosol-assisted sol-gel process